Ordering Kinetics of the BCC Morphology in Diblock Copolymer Solutions over a Wide Temperature Range

Zhizhong Liu[†] **and Montgomery Shaw***[,†,‡]

Department of Chemical Engineering and Polymer Program of The Institute of Material Science, U-3136, University of Connecticut, Storrs, Connecticut 06269

Benjamin S. Hsiao

Department of Chemistry, State University of New York at Stony Brook, Stony Brook, New York 11794-3400

Received July 29, 2004; Revised Manuscript Received September 28, 2004

ABSTRACT: The morphology and order-to-disorder transition (ODT) of solutions of a low molecular weight poly(styrene-*b*-ethylene-*alt*-propylene) in squalane were studied by four different methods: DSC, modulated DSC, rheology, and small-angle X-ray scattering (SAXS). The ordering from disordered micelles to the BCC morphology was traced by both rheological and SAXS measurements. The ordering mechanism was found to follow the “nucleation and growth” pathway under both shallow and deep temperature quenches. The ordering process resembles the crystallization of semicrystalline polymers. The ordering half-time ($t_{0.5}$) showed a clear minimum at an intermediate temperature. At temperatures far below the ODT temperature (T_{ODT}) but well above the glass transition temperatures of the solvent and the corona block of the micelles, $t_{0.5}$ increased with concentration. The temperature dependence of the ordering process was analyzed using the Fredrickson−Binder theory. Following a shallow quench ($T_{\mathrm{ODT}} - T < 15$ °C), $t_{0.5}$ was found to vary with the quenching depth as $\ln t_{0.5} \propto (T_{\mathrm{ODT}} - T)^{-2}$. Following a deep quench ($T_{\mathrm{ODT}} - T > 50$ °C), the ordering time followed a simple Arrhenius relationship, and the activation energy showed negligible dependence on concentration.

Introduction

Block copolymers in the bulk or in selective solvents tend to microphase separate into diverse ordered morphologies such as lamellae, cylinders, spheres, and gyroids. The characteristic dimensions of these self-assembled morphologies are usually in the range of 10−100 nm. The relatively weak interactions and the slow relaxation of the self-assembly process often make their transition kinetics intricate and complex.[1,2] Thus, understanding of the transition kinetics of block copolymers should enable us to devise more effective pathways to manipulate nanostructures of block copolymers for varying applications.

On the basis of the fluctuation model, Fredrickson and Binder[3,4] suggested that the disorder-to-order transition (ODT) of block copolymers proceeds via a “nucleation and growth” process regardless of the quench depth. They proposed the following scaling equations to estimate the homogeneous nucleation barrier energy (ΔF^*) and the ordering half-time ($t_{0.5}$) for asymmetric diblock copolymer melts:

$$\Delta F^*/k_{\mathrm{B}}T \sim \check{N}^{1/2}|f - 0.5|^5\delta^{-2} \tag{1}$$

$$t_{0.5} \sim \check{N}^{1/12}\delta^{-3/4}\tau_{\mathrm{d}} \exp(\Delta F^*/4k_{\mathrm{B}}T) \tag{2}$$

In these equations, $\check{N} = N\alpha^6/\mu^2$ is the fluctuation term, where α and μ represent the statistical segmental length and volume, respectively; δ is a dimensionless parameter for undercooling and is defined as $(\chi - \chi_{\mathrm{ODT}})/\chi_{\mathrm{ODT}}$, where χ_{ODT} and χ are the interaction parameters at T_{ODT} and the final temperature, respectively; f is the volume fraction of one block in the melt, and τ_{d} is the copolymer terminal relaxation time. τ_{d} below T_{ODT} can be obtained by extrapolating from the relaxation times measured at temperatures above T_{ODT} or direct rheological measurements on quenched samples if the metastable disordered state lasts for a long enough time. This theory predicts that the ordering kinetics for block copolymers and the crystallization of polymer melts should be the same. Under shallow-quench conditions (close to T_{ODT}), the ordering process is nucleation-controlled. Assuming that $\chi = A/T + B$, where A and B are constants, simple mathematic manipulations lead to $\delta \propto A(1/T - 1/T_{\mathrm{ODT}}) \propto (T_{\mathrm{ODT}} - T)/T$. For shallow quenches, if $(T_{\mathrm{ODT}} - T) \ll T$, $\delta \propto (T_{\mathrm{ODT}} - T)$ is a good approximation, and the ordering time is found to have a very strong temperature dependence, i.e., $\ln t_{0.5} \sim (T_{\mathrm{ODT}} - T)^{-2}$. Under deep-quench conditions (far below T_{ODT}), the diffusion process will control the overall ordering rate. Therefore, a U-shaped temperature dependence of the ordering time is expected.

Many previous studies[5−20] of the ordering kinetics of block copolymers have confirmed the nucleation and growth mechanism. For example, experimental observations by Rosedale and Bates[5] and Floudas et al.[8,12,13] revealed the relationship $\ln t_{0.5} \propto (T_{\mathrm{ODT}} - T)^{-n}$, with n varying between 1 and 2 for several block copolymer melts subjected to a shallow quench. They also pointed out a diffusion-controlled region for the ordering of block copolymers. Recently, Floudas et al.[14] reported the dependence of the apparent T_{ODT} on the supercooling in symmetric and asymmetric block copolymers due to grains of different sizes, and an equilibrium value was obtained through the Hoffman−Weeks plot. These results established the similarity between the ordering of block copolymers and the crystallization of semicrys-

---

[†] Department of Chemical Engineering.
[‡] Polymer Program of The Institute of Material Science.

10.1021/ma0484330 CCC: $27.50

talline homopolymers. However, the slowing or immobilization of dynamics of one block at temperatures below its T_g prevented a detailed investigation of this process. In our study, this was overcome by selecting semidilute diblock copolymer solutions, where the micelles possess enough mobility at temperatures far below the T_g of the micelle core block but still well above the T_gs of the solvent and the corona block. The characteristics of the ordering process during the formation of a BCC morphology in block copolymer solutions were investigated by rheological and time-resolved small-angle X-ray scattering (SAXS) methods over a wide temperature range. The temperature and concentration dependencies of ordering rate were examined under both shallow and deep quenches.

Experimental Methods

Materials. Squalane (SQ) was purchased from Aldrich and was used without further purification. It is a hydrocarbon oil with a very high boiling temperature (>250 °C). The diblock copolymer, poly(styrene-*b*-ethylene-*alt*-propylene) (SEP20), was synthesized via cationic polymerization from styrene and isoprene monomers. The polyisoprene block was later hydrogenated and converted into poly(ethylene-*alt*-propylene). The synthesis of this material was performed by Dr. Hahn at Dow Chemicals following procedures described in a previous paper.[21] SEP20 had a $M_n = 54\,000$ and $M_w/M_n = 1.04$. In SEP20 the weight percentage of PS was 20%, and 98.7% of the double bonds in the isoprene monomeric units were saturated as characterized by proton NMR. The SEP20/SQ solutions were prepared at room temperature by mixing the desired amount of SEP20 and squalane. Tetrahydrofuran (THF) was added as a cosolvent (3:2 v/v, THF:squalane) to accelerate the dissolution. The THF was later removed first by natural evaporation in a hood for a week and then by vacuum at room temperature for about another week. Optically clear solutions were obtained at the end of sample preparation. GC-MS showed that the solutions contained less than 0.01 wt % of THF. TGA was used to confirm the nominal concentrations of 10, 15, and 20 wt % used in this study.

Rheology Measurements. The rheological properties of the block copolymer solutions were studied using an ARES instrument (Rheometric Scientific Inc., Piscataway, NJ). To ensure adequate signal-to-noise ratios, a 50 mm cone−plate ($\theta = 0.04$ rad) fixture was used. Only linear viscoelastic properties were measured, and the linear range was determined by strain sweeps. For all the three SEP20/SQ solutions, the linear region was found to be $\gamma < 0.05$. Dynamic measurements conducted in this study included isothermal time sweeps, isothermal frequency sweeps, and isochronal temperature scans.

Small-Angle X-ray Scattering. Synchrotron SAXS measurements were performed at the beamline X27C in the National Synchrotron Light Source (NSLS) Brookhaven National Laboratory (Upton, NY). The X-ray wavelength (λ) was 0.1366 nm. The distance between the sample and the imaging plate detector was 1886 mm. Exposure time for each measurement was 30 s. The scattering angle of the 2D SAXS patterns was calibrated using silver behenate; its first-order scattering vector q ($q = 4\pi \sin \theta/\lambda$, where 2θ is the scattering angle) of 1.076 nm^{-1} was used for the calibration. The linear SAXS intensity profiles were obtained by azimuthal averaging of the SAXS patterns.

Differential Scanning Calorimetry. Both conventional and temperature-modulated DSC (TMDSC) measurements were carried out to determine the phase transitions and the associated thermal changes in block copolymer solutions. Both measurements were conducted on a Q100DSC instrument from TA Instruments (Newcastle, DE). The cell calibration was performed with an indium standard, and the temperature calibration was made using indium and lead standards. A standard sapphire sample was used to calibrate the heat capacity for the modulation study. Hermetic liquid pans were used in the experiments. To maximize the formation of the ordered morphology, the SEP20/SQ solutions were annealed at a temperature about 20 °C below their T_{ODT}, which, according to the rheology measurements, maximizes the ordering rates. In this study, only the heating process was investigated. For conventional DSC measurements, a heating rate of 10 °C/min was used; for TMDSC measurements, a heating rate of 1 °C/min and a temperature modulation with the amplitude of 0.5 °C and the period of 60 s were chosen. The temperature modulation amplitude was smaller than the product of heating rate and modulation period, so there was no local cooling during the scan. This mode is referred to as "heat only" in TMDSC.

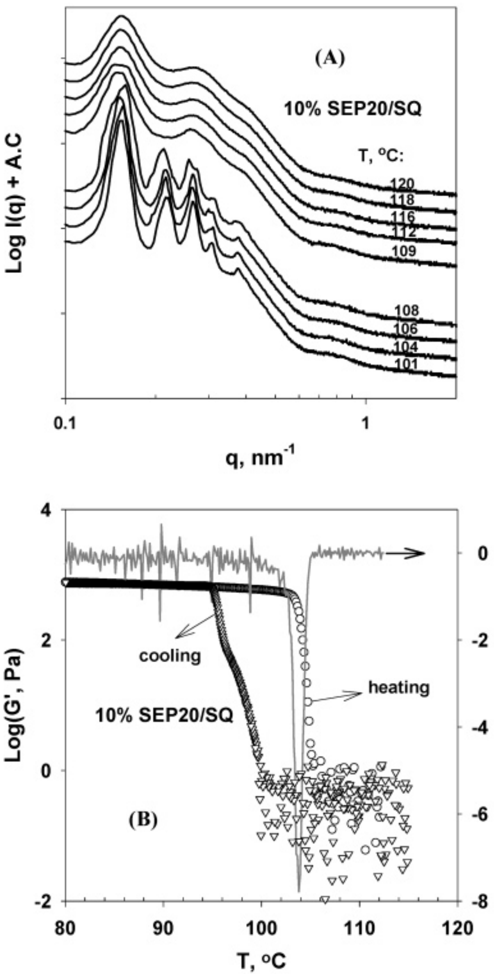

Figure 1. Measurement of T_{ODT} by (A): SAXS, 5 min hold time at each T; (B) dynamic isochronal temperature scan, $f = 1$ Hz, $\gamma = 0.02$, heating rate = 1 °C/min. Note that the derivative is dG'/dT, not d(log G')/dT.

Results and Discussion

Order-to-Disorder Transition. The as-cast SEP20/SQ solutions with concentrations from 10 to 20 wt % exhibited ordered structures as seen by SAXS measurements (Figure 1A). Frequency sweep measurements suggested a solidlike rheological behavior ($G' \gg G''$ and $G' \propto \omega^0$) in these solutions. The order-to-disorder transition temperature (T_{ODT}) of SEP20/SQ solutions was determined by three different methods: SAXS, DSC, and rheological measurements (temperature sweeps). The SAXS profiles of the solutions were measured at 2 °C increments from about 20 °C below T_{ODT} to about 10 °C above T_{ODT}, with a 5 min hold time at each temperature. As shown in Figure 1A, the five scattering peaks at the low-q range of the SAXS profiles show the ratios of the peak positions to be $1{:}\sqrt{2}{:}\sqrt{3}{:}\sqrt{4}\sqrt{}{:}\sqrt{5}$, indicating a body-centered-cubic (BCC) structure. For the 10 wt % SEP20/SQ solution, the order-to-disorder transition fell between 108 and 109 °C, as illustrated in Figure 1A by the disappearance of the higher-order scattering peaks. Even after disordering, the SAXS profiles still showed two broad peaks in the low-q range, indicating the existence of a liquidlike arrangement of micelles in the 10 wt % SEP20/SQ solution up to 120 °C. This result is consistent with previous reports,[22,23] confirming the existence of a disordered micellar region between the so-called "lattice disordering temperature" and the "micelle dissolution temperature" in block copolymer systems.

Rheological measurements have also been widely used in the determination of T_{ODT} in block copolymer systems.[5,8,11–13,22,27] Using a sinusoidal strain with $\omega = 6.28$ rad/s and $\gamma = 0.02$, the storage modulus (G') of the 10 wt % SEP20/SQ solution was measured during the heating scan from 80 to 115 °C at 1 °C/min. As depicted in Figure 1B, the order-to-disorder transition is evident by a sudden drop of G' during the heating process. Similar results were found for all concentrations used in this study. T_{ODT} was determined as the temperature where G' showed a maximum drop during heating, which can be located by the peak in the curve of the first derivative of $G'(T)$ in Figure 1B. Using this method, the T_{ODT} was found to be 104 °C for the 10 wt % SEP20/SQ solution. During cooling, the ordering process was delayed to about 5 °C below T_{ODT}, as shown by the sudden increase of G'. Also, the ordering process appeared to occur in two steps. G' exhibited a plateau value first in cooling and later recovered to its original value at low temperatures.

For asymmetric block copolymer systems, Leibler[24] and Fredrickson and Helfand[25] predicted that the order-to-disorder transition (ODT) is a first-order transition. However, distinguishing the first- and second-order transitions by rheological or SAXS measurements is rather difficult. To test whether the ODT in these block copolymer solutions is a first-order transition, thermodynamic properties such as the specific volume, heat capacity, and molar entropy should be investigated. Using conventional DSC, a heat flow or enthalpy change can be measured near the phase transition. When an endothermic or exothermic peak is observed from DSC thermograms, the corresponding transition may be considered as a first-order transition (except for the physical aging associated with the glass transition). Recently, some groups[13,18,26] observed endothermic peaks for the ODT of block copolymers in DSC experiments and reported a fusion heat of around 1−3 J/g for the ordered phases in block copolymer melts. Similar to these studies, the melting of the BCC structure in SEP20/SQ solutions also showed an endothermic peak in Figure 2A, indicating a first-order transition. The heat of fusion for the BCC structure in SEP20/SQ solutions was found to increase with the block copolymer concentration; however, its value is relatively small when compared to that of the crystalline structure in semicrystalline homopolymers. This result is consistent with previous reports on the magnitude of the enthalpy change in ODT of block copolymer melts and of concentrated solutions.[1,26]

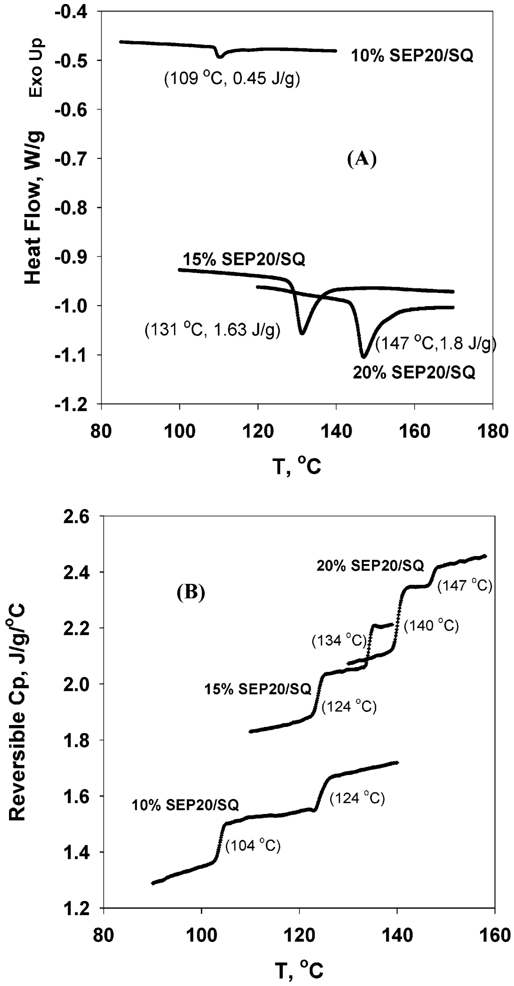

Figure 2. (A) Normal DSC measurements (heating rate = 10 °C/min). (B) Modulated DSC measurements (average heating rate = 1 °C/min; temperature modulation: amplitude = 0.5 °C, period = 60 s) for the SEP20/SQ solutions.

Temperature-modulated DSC (TMDSC)[27,28] can separate the total heat flow into a heat capacity-related (reversible) component and a kinetics-related (nonreversible) component. The reversible signal is useful for quantifying thermodynamic transitions involving a heat capacity change, while the nonreversible signal contains information about the time-dependent events in the sample. As shown in Figure 2B, during the heating process, two step-changes in the reversible heat capacity were observed for the SEP20/SQ solutions. The first change in heat capacity is very close to the lattice disordering temperature measured by SAXS and rheology experiments. The second heat capacity change at higher temperatures, which appears to increase systematically with concentration, should be related to the dissolution of the micelles in the solution, as has been predicted by Lodge et al.[23] Disordered micelles exist at intermediate temperatures between these two step-changes in the reversible heat capacity, which was confirmed by SAXS measurements in the same temperature range.

In conventional DSC or TMDSC, no changes corresponding to ordering phenomenon were observed during cooling of the solutions from temperatures above T_{ODT}. In addition, no dramatic enthalpy or heat capacity changes were observed during the reheating process, although the above results in the first heating process of a fresh sample are reproducible. This is in contrast to the rheological results shown in Figure 1B, where the disordering and ordering can be repeatedly observed

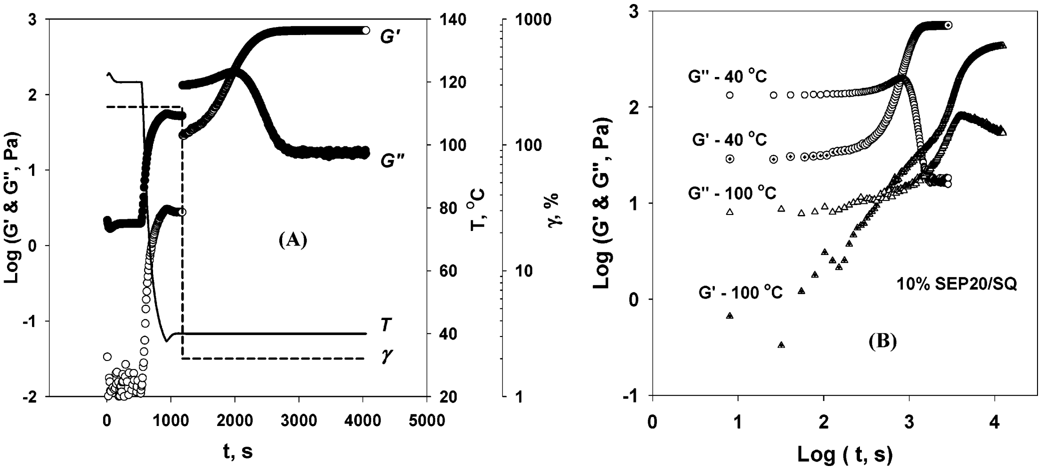

Figure 3. (A) Experimental routes for the ordering kinetics study using dynamic rheometry. (B) Evolution of the loss and storage modulus ($\omega = 6.28$ rad/s, $\gamma = 0.02$) of the 10 wt % SEP20/SQ solution during ordering at 40 and 100 °C.

Table 1. T_{ODT} (°C) of SEP20/SQ Solutions Measured by Different Methods

	concentration, wt %		
	10	15	20
TMDSC	104	124	140
DSC	109	131	147
rheology	104	121	139
SAXS	108	127	142

on the same sample during heating and cooling cycles. SAXS measurements showed the same reproducibility, although a delay of about 10 °C for the T_{ODT} was detected in the heating and cooling cycles. The reason for the unsuccessful detection of the reordering process in the cooling cycle of DSC experiments is still not clear. It might be related to the surface tension or other physical factors that can diminish the thermal effect of the phase transitions of these solutions.

The results of order-to-disorder transition measurements are summarized in Table 1. The four different techniques gave consistent results for the T_{ODT} of SEP20/SQ solutions. The T_{ODT} measured by conventional DSC (heating rate at 10 °C/min) is higher than that measured by TMDSC (average heating rate at 1 °C/min). This indicates the existence of a kinetic effect in T_{ODT} determination, probably because of the heat-transfer limitations. Another reason might be the influence of defects or grain sizes on T_{ODT} because the thermal histories of the samples in the four experimental methods were different from each other.

Ordering Kinetics and Mechanism. As indicated by the temperature (T) and strain (γ) histories depicted in Figure 3A, the ordering kinetics was studied in the following fashion: The solution was first heated to at least 15 °C above the T_{ODT} for 10 min in the rheometer fixture and was sequentially quenched to the target temperature while applying large-amplitude oscillatory shear (LAOS, $\omega = 6.28$ rad/s, $\gamma = 200\%$). After the temperature stabilized at the target point, LAOS was switched to a low strain amplitude ($\omega = 6.28$ rad/s, $\gamma = 2\%$) to trace the structural changes. A downward overshoot on the temperature curve during cooling was typically seen. Although it is unknown to what extent LAOS can destroy the ordered structures, a liquidlike rheology behavior of the solution was found in a separate frequency-sweep experiment immediately after LAOS. This result suggests, but does not prove, that a disordered state can be provided during quenching by applying LAOS simultaneously. This procedure provided a convenient way to overcome the overcooling effects on the ordering kinetics measurement of block copolymer systems, which were frequently reported in previous studies,[5-8] where extremely rapid quenches were used.

The evolution of the dynamic modulus of the 10 wt % SEP20/SQ solution during ordering is displayed in Figure 3B. At 40 °C, which is more than 60 °C below the T_{ODT}, G' showed a one-step sigmoidal increase with time, while G'' developed a maximum around the crossing point with G' and then dropped to low values. At long times, G' became much larger than G'', which is due to the formation of an elastic BCC structure.

The 2D SAXS patterns in Figure 4 show the changes of structure in the same solution after it was quenched to 40 °C from the disordered state. The micelles were disordered at the beginning as evidenced by the liquid-like scattering pattern. After 5 min at 40 °C, a continuous second-order diffraction ring was discernible. This suggests that the BCC structure began to form during the induction period of the G' curve. The random diffraction pattern implies a large number density of BCC grains in the solution. No scattering rings attributable to other ordered structures were found in the SAXS pattern or the integrated SAXS profiles. As time went on, the BCC grains coarsened, as evidenced by the increase in intensity and sharpness of the diffraction rings. Higher order diffraction rings became clearer, and some bright spots appeared on the diffraction patterns, indicating the existence of some large BCC domains relative to the beam diameter of about 1 μm.

At 100 °C, which was close to T_{ODT}, G' exhibited a distinct two-step sigmoidal increase with time, while the evolution of G'' was similar to that in the deep quench. SAXS patterns taken at 5 and 10 min after quench (Figure 5) confirmed the formation of the BCC structure during the first sigmoidal increase of G' at 100 °C (see Figure 3B). However, the discrete spots or arches instead of a continuous diffraction rings suggest the limited number of the BCC grains in the scattering volume. Judging from the SAXS patterns and the magnitude of G', the first sigmoidal step on the G' curve of the 10 wt % SEP20/SQ solution at 100 °C can be attributed to the formation of enough BCC nuclei in the disordered solution to result in changes of the rheological properties. This is in contrast with the studies by Schüler et al.,[9] Hashimoto et al.,[15] and Adams et al.[11]

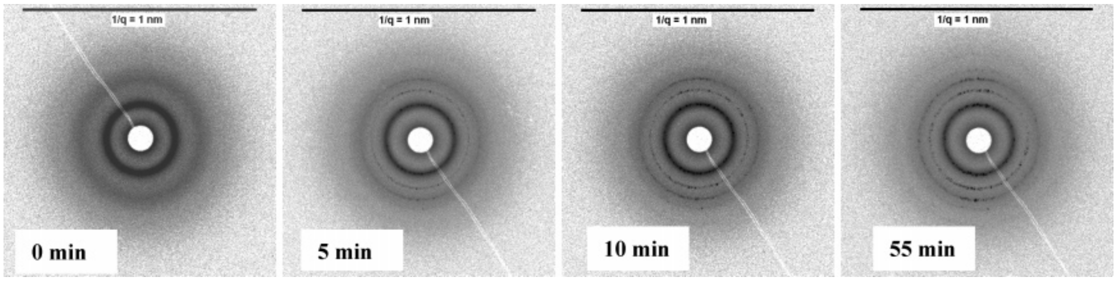

Figure 4. Evolution of SAXS patterns of 10 wt % SEP20/SQ at 40 °C after quenching from 120 °C.

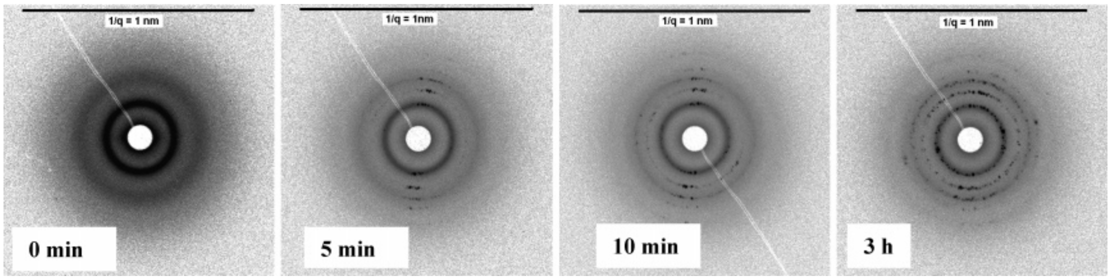

Figure 5. Evolution of SAXS patterns of 10 wt % SEP20/SQ at 100 °C after quenching from 120 °C.

concerning the presence of fast and slow modes during the quiescent ordering of block copolymer melts. They related the fast mode to the microphase separation and associated the slow mode with the development of long-range order. However, for the ordering of 10 wt % SEP20/SQ solution, SAXS experiments (Figure 1A) showed that micelles were still present at 120 °C, the temperature used to disorder the solution. Thus, the first sigmoidal increase of G' in Figure 3B cannot be attributed to the formation of micelles or microphase separation. On the other hand, the lack of the first sigmoidal step in the G' curve at 40 °C might be related to fast nucleation at low temperatures since the nucleation barrier has an inverse quadratic relationship with quench depth according to eq 1. In this case, although many BCC nuclei form immediately after the quench, their effect on the rheological properties is not profound. The increase of the size of the ordered domains and the elimination of the lattice defects during the coarsening process are likely to be responsible for the change of rheological properties during ordering. At long annealing times, when the G' curve leveled off, the SAXS patterns displayed both diffusive and discrete scattering features in both deep and shallow quenches, indicating the coexistence of the disordered and the ordered structures in SEP20/SQ solutions even after the completion of the ordering process.

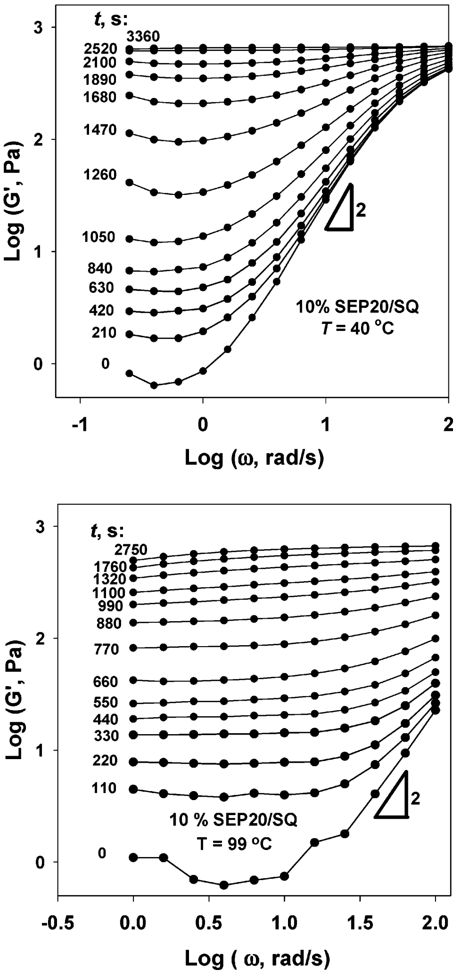

Figure 6. Evolution of the G' frequency spectrum after quenching the 10% SEP20/SQ from 120 °C to 40 and 99 °C.

Frequency-sweep measurements provided further information on the evolution of structure during the ordering of the micelles following the quench from the disordered state. Figure 6 shows the frequency dependence of G' taken at time intervals of 210 and 110 s for the ordering process of the 10 wt % SEP20/SQ solution at 40 and 99 °C, respectively. The frequency sweeps were conducted from high to low frequency using the quenching procedure depicted in Figure 3A. Because the measurement for each data point required a time allocation of $2\pi/\omega$, the high-frequency data could be considered quasi-static. In contrast, the low-frequency data are undoubtedly influenced by aging effects. For the ordering of the 10 wt % SEP20/SQ solution, the evolution of the G' frequency response followed a similar pattern after both shallow (99 °C) and deep (40 °C) quenches. The G' frequency response showed a terminal flow behavior ($G' \propto \omega^2$) for the disordered micelles at the early stage of ordering. But even in the early stage, the formation of the BCC clusters or grains was evident by an upward tail at low frequencies (longer measuring time) following the terminal region of the $G'(\omega)$ curve; otherwise, the terminal behavior would have extended

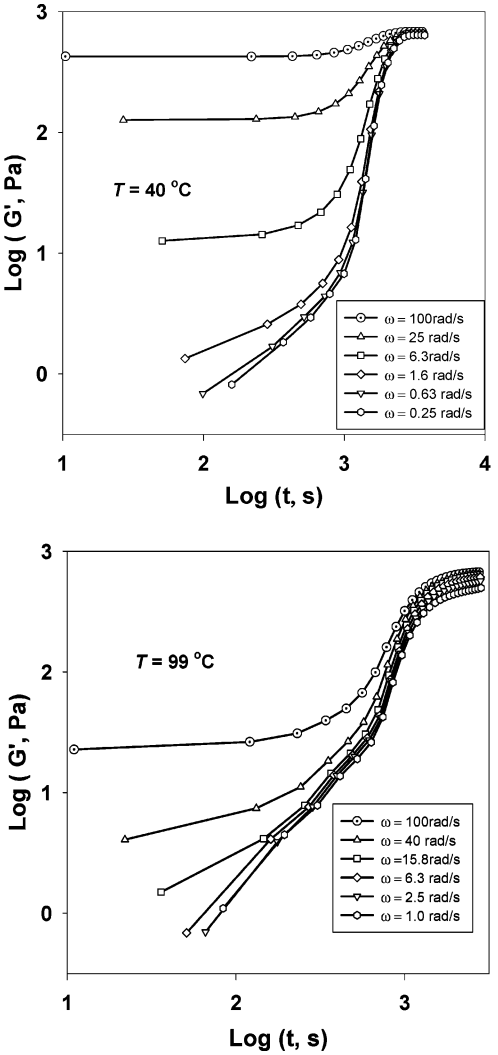

Figure 7. Evolution of G' at different frequencies after quenching the 10% SEP20/SQ from 120 °C to 40 and 99 °C. G' data are extracted from the quasi-static frequency sweeps in Figure 6.

to the lowest frequency of our experimental window. This result is consistent with the SAXS observation that the ordered BCC morphology appeared in the solution almost immediately after quench (less than 5 min). As time went on, the storage modulus kept increasing and became less frequency dependent. At long times, the storage modulus became almost frequency-independent in the whole experimental window and changed little with time, signifying the completion of the ordering process.

A careful examination of the data from Figure 6 showed that the shape of the $G'(t;T)$ aging response is actually frequency-dependent. As illustrated in Figure 7, after both shallow and deep quenches G' measured at high frequencies (e.g., $\omega = 100$ rad/s) showed a one-step sigmoidal increase with time, while a two-step sigmoidal increase with time is discernible for the G' measured at low frequencies (e.g., $\omega = 0.25$ rad/s at 40 °C, $\omega = 1.0-6.3$ rad/s at 99 °C). These observations, combined with the SAXS results (Figures 4 and 5), suggest that the observed ordering behavior (e.g., one-step vs two-step) by rheological methods is dependent on both temperature and frequency. At a fixed frequency (e.g., 6.28 rad/s in Figure 3B), only particles (micelle clusters or BCC nuclei) with large enough size will contribute to the measured storage modulus. Following a deep quench, the G'-contributing particles (BCC nuclei) have relatively smaller size, and these small nuclei form almost instantly because of the low nucleation barrier in this case. For this reason, the nucleation process following a deep quench is not resolvable using this specific frequency. Using the same frequency, following a shallow quench the G'-contributing BCC nuclei have much larger sizes because of the improved particle mobility with temperature. In this case, since the nucleation barrier is higher, it takes much more time to form the larger BCC nuclei; thus, the nucleation process becomes observable with this frequency, and a two-step sigmoidal increase appears in the $G'(t)$ curve.

Critical gel behavior, which is a common phenomenon in the liquid-to-solid transition (LST) of polymers,[30] was not observed in the ordering of SEP20/SQ solutions, although the ordering of the disordered micelles into a BCC morphology is a legitimate liquid-to-solid transition. Critical gel behavior is due to the self-similarity of the relaxation modes over a wide range of relaxation times for fractal network structures formed near a LST by either chemical or physical cross-linking. The distinguishing rheological behavior is that G' and G'' follow the same power-law dependence on frequency. This characteristic was not observed in the frequency sweeps during the ordering process of SEP20/SQ solutions following either a deep or a shallow quench. Unlike triblock copolymers, where the bridging blocks provide attractive connectivity among different microdomains, the only possible connectivity in diblock copolymer systems is through the entanglement of the matrix blocks in melts or the entanglement of micelle corona chains in solutions. These topological restrictions can easily relax. Critical gel behavior has been observed in the ordering process of triblock copolymers in both melts and solutions.[17,31] For diblock copolymers, however, the longest relaxation time does not diverge to infinity even for the ordered state in melts. Register et al.[32,33] and Bates et al.[34] recently reported a terminal flow for the cubic structures formed in diblock copolymer melts at very low frequencies. The mechanism for stress relaxation is through the sliding of the ordered domains on the boundaries or the diffusion of defects. On the other hand, critical gel scaling behavior of $G' \sim G'' \sim \omega^{1/3}$ and $G' \sim G'' \sim \omega^{1/2}$ has been observed for the hexagonally packed cylindrical (HCP) and lamellar phases in block copolymer systems, respectively.[34] The HCP and lamellar structures are liquid crystal structures, which can flow and relax stresses along the cylindrical axis or the lamellar planes, respectively, but they behave as a solid in the other directions. Thus, for a polycrystalline HCP or lamellar phase, the percolation of these highly anisotropic self-assembly particles leads to a critical gel-like behavior.

Avrami Fitting. To simplify the presentation, the evolution of complex modulus magnitude, $|G^*| = [(G')^2 + (G'')^2]^{1/2}$, was used to represent the ordering process of the SEP20/SQ solutions. In Figure 8A, it is seen that the ordering process of the 10 wt % SEP20/SQ solution accelerates with temperature from 40 to 80 °C, while in Figure 8B the process slows down with temperature from 90 to 100.5 °C. To analyze the ordering kinetics over the full temperature range, a "parallel" mechanical model[35] was used to extract the time-dependent volume fraction, $\phi(t)$, of the ordered phase. Then the Avrami equation was fitted to the $\phi(t)$ data to provide kinetic

Table 2. Avrami Fitting Parameters for the Ordering of 10% SEP20/Squalane Solution

	T, °C																	
	40	45	50	55	60	65	70	75	80	90	94	95	96	97	98	99	100	100.5
$\|G^*_i\|$, Pa	143	117	95	78	61	52	40	34	31	19	16	14	14	14	13	13	12	9
$\|G^*_f\|$, Pa	706	738	771	794	765	777	769	774	794	762	713	648	637	637	612	612	433	239
n	3.8	4.2	4.6	5.0	5.1	5.3	5.4	5.6	5.6	5.7	5.4	6.0	6.0	5.5	4.4	3.0	2.3	1.0
τ, s	1100	828	615	406	235	154	135	119	79	102	157	263	296	318	382	852	4800	46400

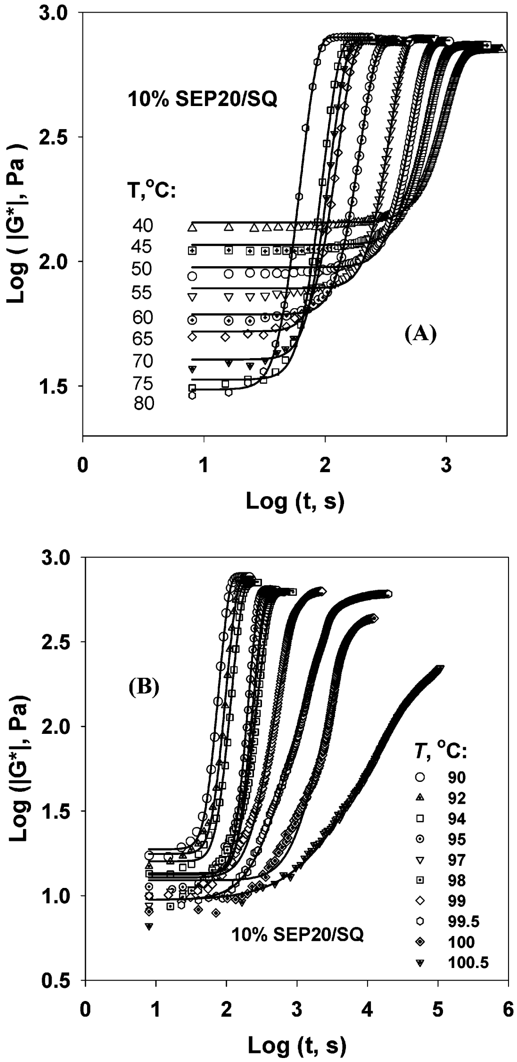

Figure 8. Evolution of the complex modulus magnitude (ω = 6.28 rad/s, γ = 2%) during the ordering process of 10% SEP20/squalane solution at different temperatures after quenches from 120 °C with LAOS (ω = 6.28 rad/s, γ = 200%): (A) low-temperature range; (B) high-temperature range.

information. The parallel model and the Avrami equation can be expressed as

$$|G^*(t)| = G_i^*|[1 - \phi(t)] + |G_f^*|\phi(t) \tag{3}$$

$$\phi(t) = 1 - \exp[-(t/\tau)^n] \tag{4}$$

where $|G_i^*|$ and $|G_f^*|$ are the initial and equilibrium modulus, respectively; τ is a time constant corresponding to 63.2% of conversion, and n is the Avrami exponent. Combining these two equations yields

$$|G^*(t)| = [|G_f^*| - |G_i^*|]\{1 - \exp[-(t/\tau)^n]\} + |G_i^*| \tag{5}$$

The Avrami fits using eq 5 are shown as the lines in Figure 8A,B. The fitting curves match very well with the experimental data except for the high-temperature cases close to T_{ODT}, where the two-step sigmoidal behavior occurs.

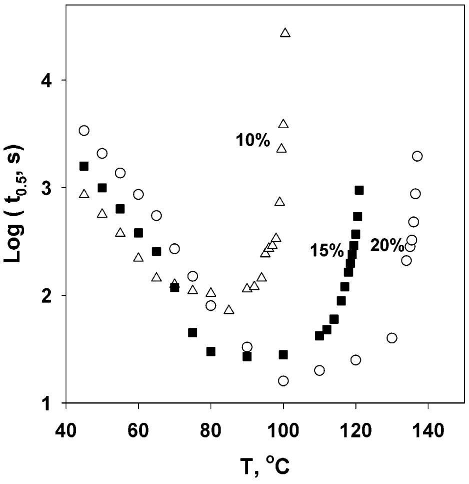

Figure 9. Ordering half-time ($t_{0.5}$) of SEP20/SQ solutions with concentration at 10, 15, and 20 wt %.

The fitting results are summarized in Table 2. Although the initial modulus of the disordered state decreased steadily with temperature, the equilibrium modulus of the ordered state was found to increase first with temperature and then decrease. The Avrami exponent increased first from about 4 to 6 and then dropped quickly to 1 as the temperature approached T_{ODT}. The ordering time, indicated by τ, decreased with temperature first and reached a minimum around 80 °C; it then increased dramatically with temperature near T_{ODT}.

The ordering kinetics over a wide range of temperatures for the other two SEP/SQ solutions (15 and 20 wt %) was studied in a similar way. The ordering half-time $t_{0.5}$ can be obtained by $t_{0.5} = \tau(\ln 2)^{1/n}$ and compared with the Fredrickson–Binder theory. The temperature dependence of $t_{0.5}$ for the three SEP20/SQ solutions is depicted in Figure 9. A U-shaped temperature dependence can be identified for the ordering of SEP20/SQ solutions, similar to that of the crystallization process in polymer melts.[28] In accordance with the theoretical prediction by Fredrickson and Binder,[3,4] the increase of $t_{0.5}$ with temperature near T_{ODT} can be attributed to the dominance of the nucleation effects, while the decrease of $t_{0.5}$ with temperature in the low-temperature range can be attributed to the dominance of the diffusion effects. The competition of these two effects on the ordering kinetics results in the U-shaped temperature dependence and the appearance of a minimum point for the ordering time.

The temperature dependence of $t_{0.5}$ at low temperatures (from 40 to 65 °C) is shown Figure 10A; the straight line in the Arrhenius plot indicates the following relationship.

$$t_{0.5} \propto \exp(\Delta E/RT) \tag{6}$$

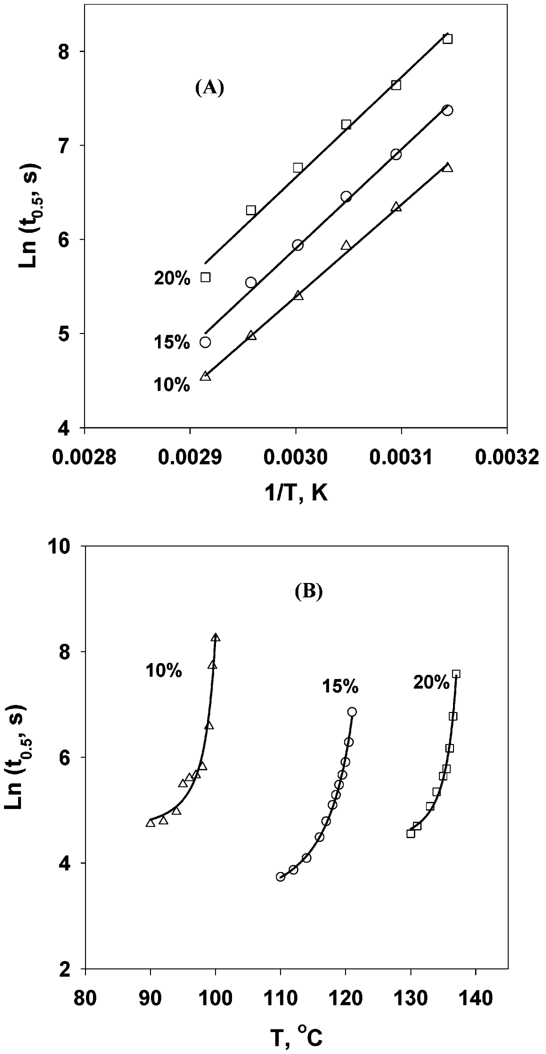

Figure 10. (A) Arrhenius plot of the ordering half-time for SEP20/squalane solutions from 45 to 70 °C. (B) Temperature dependence of ordering half-time near T_{ODT}. The lines are fits with eq 7.

Here ΔE is the apparent activation energy for the ordering, which was found to be 88.6 ± 4.7, 87.7 ± 3.1, and 81.5 ± 1.9 kJ/mol for the 10, 15, and 20 wt % SEP20/SQ solutions, respectively. On the other hand, in Figure 10B, the ordering half-time at high temperatures ($T_{\text{ODT}} - T < 15$ °C) displays a much stronger temperature dependence in accordance with the Fredrickson−Binder theory:

$$\ln t_{0.5} = A(T_{\text{ODT}} - T)^{-2} + C \tag{7}$$

where A and C are constants. By fitting the experimental data to this equation, T_{ODT} was found to be 103.4 ± 0.8, 129.3 ± 0.7, and 140.5 ± 0.4 °C, respectively, for the 10, 15, and 20 wt % SEP20/SQ solutions. The extrapolated T_{ODT} is very close to the experimentally measured value by different methods (Table 1). A was found to be 43.7 ± 21.8, 260.1 ± 46.6, and 39.2 ± 9.6 K^2, whereas C was found to be 4.6 ± 0.2, 3.0 ± 0.1, and 4.3 ± 0.1 for the 10, 15, and 20 wt % SEP20/SQ solutions, respectively. These results indicate that Fredrickson−Binder's theory assuming a homogeneous nucleation process for the ordering of asymmetric block copolymer melts can also be applied to the ordering of block copolymer solutions near ODT.

Conclusion

The order-to-disorder transition of the BCC morphology in diblock copolymer solutions was characterized by four methods: rheology, DSC, TMDSC, and SAXS. Disordered micelles were observed after the melting of the ordered BCC structure. The ordering of the disordered micelles after quenching from temperatures above T_{ODT} followed a nucleation and growth mechanism over a wide temperature range. The ordering half-time showed a minimum at intermediate temperatures. After a deep quench, the ordering process is apparently diffusion-controlled; the ordering times decreased with temperature and followed the Arrhenius relationship. Following a shallow quench, the ordering process is apparently nucleation-controlled; the ordering times increased with temperature, and it could be qualitatively described by the theory of Fredrickson and Binder assuming a homogeneous nucleation mechanism.

Acknowledgment. SAXS measurements were done in the X27C beamline (supported by Department of Energy DE-FG02-99ER 45760) at the National Synchrotron Light Source, Brookhaven National Lab, with the kind assistance of Dr. Carlos Avila. This work was supported in part by STP Corp.

References and Notes

(1) Hadjichristidis, N.; Pispas, S.; Floudas, G. A. *Block Copolymers: Synthesis Strategies, Physical Properties and Applications;* Wiley-Interscience: New York, 2003; p 313.
(2) Lodge, T. P. *Macromol. Chem. Phys.* **2003**, *204*, 265.
(3) Fredrickson, G. H.; Binder, K. *J. Chem. Phys.* **1989**, *91*, 7265.
(4) Binder, K. *Physica A* **1995**, *213*, 118.
(5) Rosedale, J. H.; Bates, F. S. *Macromolecules* **1990**, *23*, 2329.
(6) Harkless, C. R.; Singh, M. A.; Nagler, S. E.; Stephenson, G. B.; Jordan-Sweet, L. J. *Phys. Rev. Lett.* **1990**, *64*, 2285.
(7) Singh, M. A.; Harkless, C. R.; Nagler, S. E.; Ghosh, S. S. *Phys. Rev. B* **1993**, *47*, 8425.
(8) Floudas, G.; Hadjichristidis, N.; Latrou, H.; Fischer, E. W. *Macromolecules* **1994**, *27*, 7735.
(9) Schüler, M.; Stühn, B. *Macromolecules* **1993**, *26*, 112.
(10) Hashimoto, T.; Sakamato, N. *Macromolecules* **1995**, *28*, 4779.
(11) Adams, J. L.; Quiram, D. J.; Graessley, W. W.; Register, R. A.; Marchand, G. R. *Macromolecules* **1996**, *29*, 2929.
(12) Floudas, G.; Vlassopoulos, D.; Hadjichristidis, N.; Pakula, T.; Stamm, M. J. *J. Chem. Phys.* **1996**, *105*, 2083.
(13) Floudas, G.; Vlassopoulos, D.; Hadjichristidis, N.; Likhtman, A.; Semenov, A. *J. Chem. Phys.* **1997**, *106*, 3318.
(14) Floudas, G.; Pakula, T.; Velis, G.; Sioula, S.; Hadjichristidis, N. *J. Chem. Phys.* **1998**, *108*, 6498.
(15) Sakamato, N.; Hashimoto, T. *Macromolecules* **1998**, *31*, 3292.
(16) Sakamato, N.; Hashimoto, T. *Macromolecules* **1998**, *31*, 3815.
(17) Sakamato, N.; Hashimoto, T. *Macromolecules* **1998**, *31*, 8493.
(18) Soenen, H.; Berghmans, H.; Winter, H.; Overbergh, N. *Polymer* **1997**, *38*, 5653.
(19) Garetz, B. A.; Newstein, M. C.; Balsara, N. P. *J. Polym. Sci., Part B: Polym. Phys.* **2001**, *39*, 2231.
(20) Liu, Z.; Chattopadhyay, S.; Shaw, M. T.; Hsiao, B. *J. Polym. Sci., Part B: Polym. Phys.* **2004**, *42*, 1496.
(21) Mani, S.; Weiss, R. A.; Hahn, S. F.; Williams, C. E.; Cantino, M. E.; Khairallah, L. H. *Polymer* **1998**, *39*, 2023.
(22) Han, C. D.; Vaidya, N. Y.; Kim, D.; Shin, G.; Yamaguchi, D.; Hashimoto, T. *Macromolecules* **2000**, *33*, 3767.
(23) Dormidontova, E. E.; Lodge, T. P. *Macromolecules* **2001**, *34*, 9143.
(24) Leibler, L. *Macromolecules* **1980**, *13*, 1602.
(25) Fredrickson, G.; Helfand, E. J. *Chem. Phys.* **1987**, *87*, 697.

(26) Kim, J. K.; Lee, H. H.; Jeong, Y. H. *Macromolecules* **1998**, *31*, 4045.
(27) Scherrenberg, R.; Mathot, V.; Steeman, P. *J. Therm. Anal.* **1998**, *54*, 477.
(28) Danley, R. L. *Thermochim. Acta* **2003**, *402*, 91.
(29) Long, Y.; Shanks, R. A.; Stachurski, Z. H. *Prog. Polym. Sci.* **1995**, *20*, 651.
(30) Winter, H. H.; Mours, M. *Adv. Polym. Sci.* **1997**, *134*, 165.
(31) Sato, T.; Watanabe, H.; Osaki, K. *Macromolecules* **2000**, *33*, 1686.
(32) Sebastian, J. M.; Lai, C.; Graessley, W. W.; Register, R. A. *Macromolecules* **2002**, *35*, 2707.
(33) Sebastian, J. M.; Lai, C.; Graessley, W. W.; Register, R. A.; Marchand, G. R. *Macromolecules* **2002**, *35*, 2700.
(34) Kossuth, M. B.; Morse, D. C.; Bates, F. S. *J. Rheol.* **1999**, *43*, 167.
(35) Floudas, G.; Pakula, T.; Fischer, E. W.; Hadjichrististidis, N. *Acta Polym.* **1994**, *45*, 176.

MA0484330